FOUR IN ONE: A NEW CREVASSE-SPLAY COMPLEX IN THE MIDDLE MIOCENE OF CENTRAL POLAND

Marek WIDERA[1]*, Mariusz DZIAMARA[2], Jakub KLĘSK[1] & Robert WACHOCKI[2]

[1] *Institute of Geology, Adam Mickiewicz University, Krygowskiego 12, 61-680 Poznań, Poland; e-mails: widera@amu.edu.pl, jnklesk@gmail.com*
[2] *Konin Lignite Mine, 600-lecia 9, 62-540 Kleczew, Poland; e-mails: dziamara.mariusz@kwbkonin.pl, robert.wachocki@vp.pl*
** Corresponding author*

Widera, M., Dziamara, M., Klęsk, J. & Wachocki, R., 2024. Four in one: a new crevasse-splay complex in the middle Miocene of central Poland. *Annales Societatis Geologorum Poloniae*, 94: 1–18.

Abstract: This article focuses on a newly identified set of crevasse splays in the lignite-bearing Miocene of Poland. The sand bodies studied are situated within the First Mid-Polish Lignite Seam (MPLS-1) in the Tomisławice opencast mine, located near Konin in central Poland. The sand bodies form an alluvial complex of four superposed crevasse splays, separated by lignite layers, 0.1–0.8 m thick. They are considered to be overbank lateral splays, emplaced laterally by a fluvial channel, rather than its terminal splays. Their combined thickness reaches ~5 m, their length is <0.6 km and width <0.4 km, and their total area is ~0.1 km^2. Nearly half of the sediments examined are subaerial deposits, while the rest are typical of crevasse-splay microdeltas, accumulated in a floodplain subaqueous environment. The sand bodies with local clay lenses are both underlain and overlain by, as well as interbedded with a range of lignite lithotypes, representing various sub-environments of a mid-Miocene mire (backswamp) realm. The estimated time span for the formation of the entire-crevasse-splay complex, recording four short-term floods, is at least 48 kyr. The crevasse-splay complex is one of the best developed in lignite/coal successions worldwide. However, it poses a major technical obstacle to mining activity in the Konin Lignite Mine.

Key words: Alluvial system, backswamp, Konin Basin, lignite seam, mire, Neogene, overbank sedimentation.

Manuscript received 26 September 2022, accepted 15 November 2023

INTRODUCTION

Crevasse splays are typical overbank (extra-channel) deposits, present in all alluvial systems, particularly common on the floodplains of meandering and anastomosing rivers (Makaske, 2001; Miall, 2006; Boggs, 2012; Zieliński, 2014). They form adjacent to the margins of river channels, when the natural levees are locally breached by floodwater. The accumulation of sediments, mainly sand, takes place during the initial stage of a flood. Coarser sediment fractions (medium and fine sands) are deposited closer to the river channel, in the proximal zone of spill-out, while finer fractions (if present) tend to be deposited farther away, in the distal zone of the floodplain (e.g., Smith *et al*., 1989; Bristow *et al*., 1999; Burns *et al*., 2017, 2019).

Crevasse-splay sand bodies vary widely in size, shape and thickness. They can cover an area from hundreds of m^2 to over 20 km^2, being >10 km long and >5 km wide. Complexes of multiple crevasse-splays with compensational stacking may have an areal extent of more than 220 km^2 (Rahman *et al*., 2022a). Their shape in plan view may be lobate or dendritic, while in cross-section they are always wedge- and/or lens-shaped. The thickness of crevasse-splay sand bodies also can vary over a wide range, from a few cm to over 20 m (O'Brien and Welles, 1986; Mjøs *et al*., 1993; Farrell, 2001; Bridge, 2003; Miall, 2006; Cahoon *et al*., 2011; Gulliford *et al*., 2014, 2017; Millard *et al*., 2017; Rahman *et al*., 2022b).

The deposits of crevasse-splay complexes on an outcrop scale may resemble those of the terminal splays, formed at the downstream mouths of rivers in dry to hyper-arid or humid to tropical environments, such as the modern inland Okavango Delta in Botswana or the fluvial Kosi Fan in India (e.g., Fisher *et al*., 2008; Chakraborty *et al*., 2010; Horner *et al*., 2018). However, such 'inland deltas' are virtually dominated by terminal splays and their regional-scale depositional settings are different from those in the present case. The area of terminal splays is much larger (>2.7 km^2) than that of the lateral splays in the Miocene lignite deposits, in central Poland (generally <0.63 km^2 and ~0.1 km^2 in the present case). The relatively small lignite deposits in Poland occur patchily between the palaeochannels of an anabranching distributive fluvial system. Solitary or complex clinothemic crevasse-splay sand bodies occur on either side of the peat-forming floodplain palaeo-lakes (Widera *et al.*, 2022, 2023). Unfortunately, the lignite-devoid channel-belt sand bodies are little exposed, as they are carefully circumvented by mining activity as being non-economic.

The deposition of crevasse splays has been studied extensively in modern fluvial and deltaic environments (e.g., Zwoliński, 1985, 1992; Cloyd *et al*., 1990; Reading and Collinson, 1996; Baeteman *et al*., 1999; Bristow *et al*., 1999; Szponar, 2000; Farrell, 2001; Gębica and Sokołowski, 2001, 2002; Makaske, 2001; Bos *et al*., 2009, 2012; Kordowski *et al*., 2014; Lepre, 2017). Crevasse splays have also been documented in the rock record in coal-barren (e.g., Kraus and Wells, 1999; Burns *et al*., 2017, 2019; Gulliford *et al*., 2017; Rahman *et al*., 2022a, b) and coal/lignite-bearing successions (e.g., Horne *et al*., 1978; Flores, 1981; Guion, 1984; Fielding, 1984; Flores and Hanley, 1984; McCabe, 1984; Jorgensen and Fielding, 1996; Diessel *et al*., 2000; Davies-Vollum and Kraus, 2001; Bridge, 2003; Rajchl and Uličny, 2005; Rajchl *et al*., 2008; Davies-Vollum *et al*., 2012).

Ancient crevasse splays in Polish coal-bearing successions have been documented from the Carboniferous of the Upper Silesia Coal Basin, including the Brynów Brickyard in Katowice (Brzyski *et al*., 1976) and coal-mine exploration boreholes (e.g., Gradziński *et al*., 1995, 2005; Doktor, 2007; Kędzior *et al*., 2007; Kędzior, 2016). Crevasses and crevasse splays have been recognized also in the outcrops and mining galleries of the Namurian in the Lower Silesia Wałbrzych Coal Basin (Nemec, 1984); in the Sołtyków outcrop of the Lower Cretaceous, near Skarżysko-Kamienna in central Poland (Pieńkowski, 2004a, b); and in the lignite-bearing Miocene successions in the Polish Lowlands (Kasiński, 1986, 1989; Kramarska *et al*., 2015). The opencast study area of the 'Tomisławice' lignite deposit (Fig. 1) is the second Polish site of the lignite-bearing Miocene, where crevasse-splay sediments were uncovered in 2015 (Widera, 2016a, 2017; Widera *et al*., 2017a; Chomiak, 2020). The opencast lignite mines, based on shallow boreholes, have carefully avoided non-economic clastic deposits, but as the mining activity expanded laterally, they inevitably began to encounter such materials. Some of them, such as the local crevasse splays, were unexpected. In the last few years (2018–2021), several crevasse splays became available for direct observation in the opencasts (Jóźwin IIB, Tomisławice) of the Konin Lignite Mine (Chomiak *et al*., 2019; Wachocki *et al*., 2020; Widera, 2020; Dziamara *et al*., 2022, 2023; Widera *et al*., 2022, 2023). It seemed that the limiting of lignite mining in the Konin region would prohibit exposure of any additional crevasse splays of scientific interest. However, the crevasse-splay complex described here was encountered unexpectedly in a floodplain setting in mid-2022.

The main goal of the present study is to introduce the reader to the stratigraphic and depositional architecture of this crevasse-splay complex, the best developed, not only in the lignite-bearing Miocene of Poland, but perhaps worldwide. The study-specific aims were: (i) to map the shape, size and thickness of the crevasse-splay complex in cross-sectional and plan view; (ii) to characterize sedimentologically its component facies and the accompanying lignite lithotypes; (iii) to estimate the time span for accumulation of the entire complex; and (iv) to discuss the environmental formative conditions and uniqueness of the complex studied on both Polish and global scales.

GEOLOGICAL SETTING

The Tomisławice lignite opencast mine, operating on a lignite deposit of the same name, is located ~30 km north-northeast of the town of Konin, in central Poland. The SSE-NNW elongation of this deposit is consistent with the lowering of the Mesozoic top and the orientation of the hosting tectonic graben (Fig. 1). The present study area is in its middle part and covers the fault-bounded, shallow graben, up to 20–30 m in depth. Tectonically, the graben is in the northeast territory of the Konin Elevation (Widera, 1998, 2022), which constitutes the central part of the Mogilno Trough and the middle segment of the Szczecin-Miechów Synclinorium (Żelaźniewicz *et al*., 2011). The 'Tomisławice' lignite deposit with the crevasse-splay sand bodies studied is in the central part of an extensive mid-Miocene sedimentary basin, with an area of > 70,000 km^2 (cf. Widera, 2021).

The oldest rocks drilled in the study area are marls and calcareous sandstones of Late Cretaceous age, representing the top of the Mesozoic succession (Dadlez *et al*., 2000). They are strongly fractured and locally faulted (Fig. 2). The Cenozoic succession is discontinuous, containing long-term stratigraphic gaps. These hiatuses, related to the regional tectonic uplift and periodical predominance of erosion in central Poland, formed over three main time intervals: the latest Cretaceous–latest Eocene, the late Oligocene, and the late early Pliocene–early Pleistocene. The Paleogene is represented exclusively by marine glauconite sands of early Oligocene age (Fig. 2; Widera, 2021).

In the area of the 'Tomisławice' lignite deposit, the Neogene comprises the Koźmin Formation (lower–middle Miocene), overlain by the Poznań Formation (middle Miocene–lowest Pliocene). The Koźmin Formation consists mainly of fluvial sands, coaly (carbonaceous) sands, and thin (<1 m thick) lignite lenses. These sediments underlie the First Mid-Polish Lignite Seam (MPLS-1), mined in the Tomisławice opencast (Figs 2, 3) and containing the crevasse-splay complex studied. The Poznań Formation traditionally is divided into the lower Grey Clay Member and the upper Wielkopolska Member (Piwocki and Ziembińska-Tworzydło, 1997; Widera, 2007). This first lithostratigraphic member is complete, while the second member was strongly eroded in the Pleistocene in the study area of the 'Tomisławice' deposit (Fig. 2), although it is present as relics in other areas. In general, the Poznań Formation here comprises the MPLS-1 (up to 11.8 m thick, mean 6.9 m), enveloping the crevasse-splay complex (up to 5 m thick), with the remnant so-called 'grey clay' and 'green clay' and 'flamy clay' on top (see Appendix).

The origin of the Grey Clay Member is associated with the mid-Miocene palustrine environment, that is, a mire-lake system (Kasiński, 1986, 1989; Piwocki and Ziembińska-Tworzydło, 1997; Widera, 2007; Chomiak *et al*., 2020). The Wielkopolska Member accumulated between the late

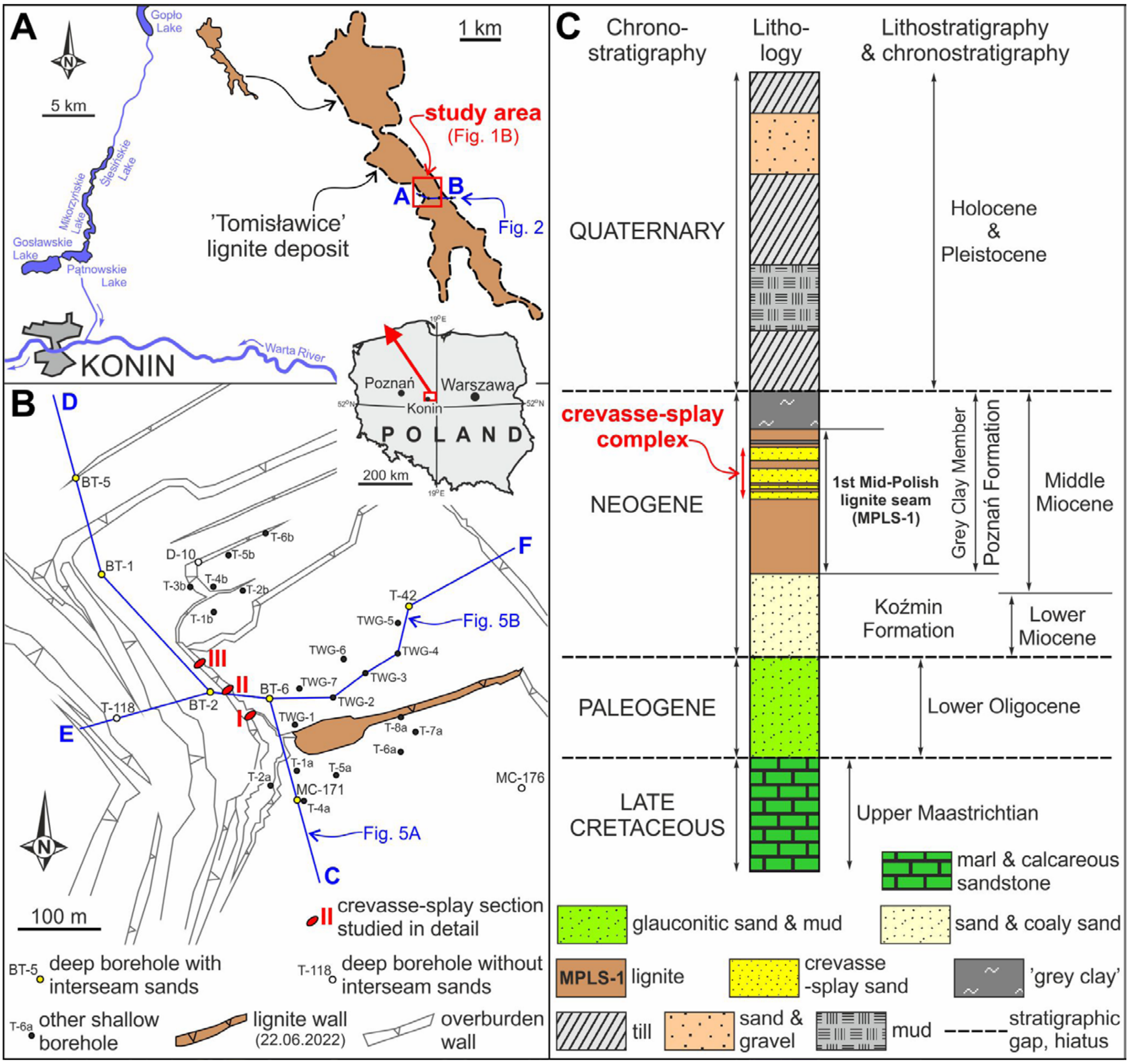

Fig. 1. Location map and simplified stratigraphy of the study area. **A.** The 'Tomisławice' lignite deposit in central Poland. **B.** Northern part of the Tomisławice opencast with outcropping crevasse-splay sediments. **C.** Generalized chrono- and lithostratigraphy in the area of the 'Tomisławice' lignite deposit. Note the location of the geological cross-section A–B in Figure 1A, as well as the geological cross-sections C–D and E–F, and sections I–III, examined in detail in Figure 1B.

mid-Miocene and the earliest early Pliocene. Its origin is related to an anastomosing (Widera, 2013a; Widera *et al*., 2017b, 2019; Maciaszek *et al*., 2020) or transitional anastomosing-to-meandering river system (Zieliński and Widera, 2020; Kędzior *et al*., 2021).

The Cenozoic succession in the study area terminates upwards with mostly glaciogenic sediments of Quaternary age. Owing to Pleistocene erosional and glaciotectonic processes, they are very diverse in terms of thickness, ranging from 35 to 60 m. The Pleistocene glacial, fluvioglacial and glaciolacustrine sediments consist of tills, sands and gravels, as well as muds (Figs 2, 3; Widera, 2017; Widera *et al*., 2017a). They are covered with a thin (<1–1.5 m) layer of Holocene sediments, including sands and muds of surface streams, locally peat, and above everything the modern soil horizon.

MATERIALS AND METHODS

Fieldwork in the Tomisławice opencast was conducted in mid-2022 (June–September), with the laboratory analyses carried out in the second half of the same year. The examined sands, positioned between two benches of the exploited lignite seam (MPLS-1), were visible both in plan view and in cross-section (Figs 3, 4). In the latter case, they were available for direct observations over a distance of >200 m in a north–south direction, where they had a total thickness of 4–5 m. Three vertical sections (I–III) along the wall of this exposure were selected for further detailed sedimentological analyses (Figs 1B, 4).

The general geology of the study area is presented here on the basis of geological cross-section A–B, which was constructed using data from four deep boreholes (Figs 1A, 2).

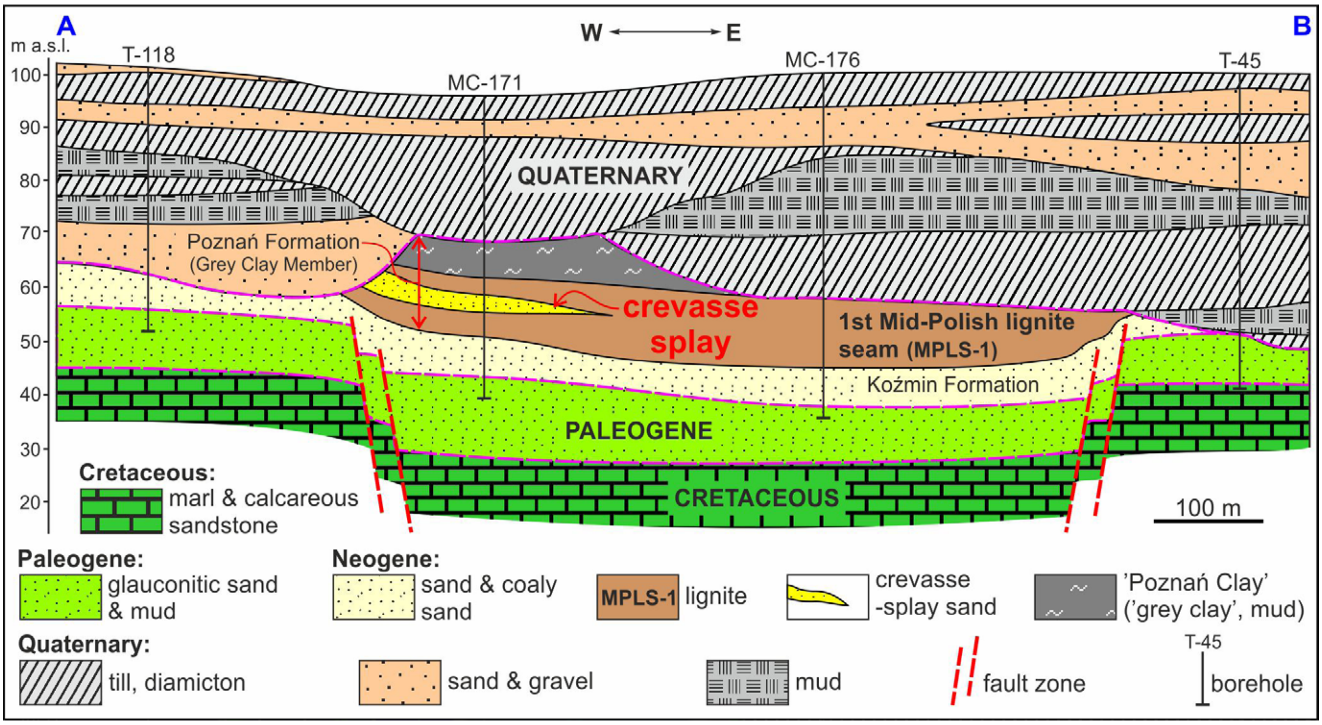

Fig. 2. Geological cross-section A–B through the middle part of the Tomisławice lignite opencast, depicting the lithology and stratigraphy of the study area. For the location of the line of cross-section A–B, see Figure 1A and for detailed chrono- and lithostratigraphy, see Figure 1C.

Fig. 3. Broad eastward view, showing the outcropping top of the examined sandy complex within the First Mid-Polish Lignite Seam (MPLS-1).

On the other hand, the cross-sections (C–D, E–F) through the sandy complex investigated, as well as thickness and structural maps of it, were constructed, using information from nine deep and 20 shallow boreholes (Figs 1B, 5, 6; Tab. 1). The deep boreholes come from older documentation of lignite reserves in the 'Tomisławice' deposit, while the shallow ones were made by the Konin Lignite Mine in early 2022 to determine the extent and thickness of the upper bench of the MPLS-1. This relatively thin (up to 1.7 m) lignite bench was selectively mined.

The sandy deposits along the outcrop sections studied in detail were described by applying the facies code of Miall (1977). For the accompanying lignite layers, the lithotype codification proposed by Widera (2012, 2016b) was used (Tab. 2; Figs 7–9). All deposits and sedimentary structures were documented photographically and 20 measurements of palaeotransport directions were based on planar cross-stratified beds (Fig. 7B); 34 samples also were collected for grain-size and organic content (burnt at 550 °C) analyses in the laboratory at the Institute of Geology,

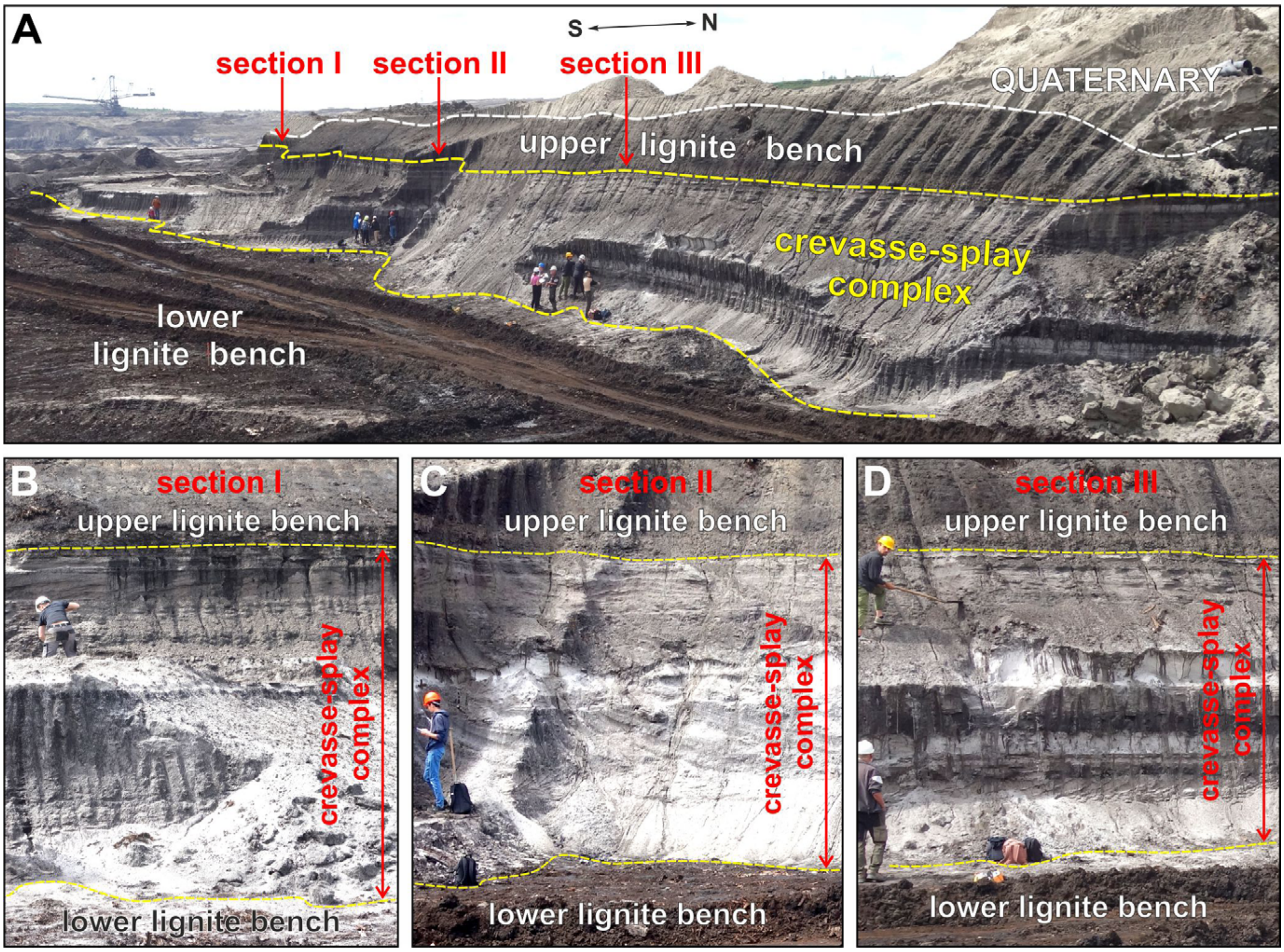

Fig. 4. General view of the sandy deposits exposed at the mining front. **A.** Broad view of the outcrop, looking towards the southwest. **B–D.** The sections I–III, studied in detail. For their location, see Figure 1B.

the Adam Mickiewicz University in Poznań, Poland (Figs 8, 9). The investigated sands were interpreted using standard facies analysis (e.g., Gradziński *et al.*, 1976; Miall, 1977, 2006; Allen, 1982; Bridge, 2003; Boggs, 2012; Zieliński, 2014), while the well-known original model of Teichmüller (1958, 1989) was applied for the characterization of lignite lithotypes.

The deposition time of the bulk sandy complex was estimated indirectly. To achieve this specific goal, the well-known accumulation time of the Main Seam from the Lower Rhine Basin (Zagwijn and Hager, 1987) and the peat-to-lignite compaction ratios for this German seam (Hager *et al.*, 1981) and for the MPLS-1 in the Konin Basin (Widera *et al.*, 2007; Widera, 2015) were compared appropriately (Fig. 10).

RESULTS

General description of the sandy complex

The sand bodies within the MPLS-1 are shown in two geological cross-sections, C–D and E–F, that are nearly meridional and latitudinal, respectively, and hence perpendicular to each other (Figs 1B, 5). The sandy complex consists of two sand bodies, the lower one being longer and thicker. It is up to 0.6 km wide and 0.4 km long, and 3.5 m thick in boreholes BT-1, BT-2, and T-42. However, the total thickness, including lignite and clay interbeds, reaches 6.5 m in borehole BT-2 (Tab. 1). In general, the sand bodies are convex upwards in cross-section C–D, and dipping eastwards and slightly concave upwards in cross-section E–F (Fig. 5).

In plan view, the complex studied is multi-fingered in shape but has similar dimensions (~0.6 × 0.4 km) along the extent of the above-described cross-sections (Figs 5, 6). Vertical sections I–III are characterized in more detail below. The total thickness of the sand bodies exceeds 4 m in the vicinity of borehole BT-2, but presumably exceeds 5 m between boreholes T-118 and BT-2, in the most proximal zone of the crevasse splays, where they were partly eroded by a Pleistocene subglacial channel (Fig. 6A). The structural map of the top of the interseam sands shows that this palaeosurface is slightly inclined, both to the south and the north, as well as to the east (Fig. 6B). This is consistent with the evidence from the geological cross-sections and the thickness distribution of the sands, confirming that the sediments were transported and deposited generally towards the eastern sector, with a slight deviation to the north (cf. Figs 5, 6).

Table 1

Basic parameters of the studied sands, used for the preparation of the cross-sections and thickness and structural maps that are shown in Figures 5, 6. For the location of the boreholes, see Figures 1B, 6.

Borehole number	Elevation of interseam sand base	Elevation of interseam sand top	Thickness of interseam sands
	[m a.s.l.]		[m]
Deep boreholes			
BT-1	56.1	59.6	3.5
BT-2	60.2	61.5	1.3
	59.5*	60.2*	0.7*
	55.0	58.5	3.5
BT-5	55.9*	56.7*	0.8*
	52.7	54.7	2.0
BT-6	58.6	59.6	1.0
	57.8*	58.6*	0.8*
	55.3	57.2	1.9
D-10	–	–	–
T-42	52.8	56.3	3.5
T-118	–	–	–
MC-171	60.1*	60.5*	0.4*
	58.5	60.1	1.8
	56.3	58.1	1.6
MC-176	–	–	–
Shallow boreholes			
T-1a	54.8	56.1	1.3
T-2a	55.2	56.9	1.7
T-4a	54.3	55.8	1.5
T-5a	53.3	54.5	1.2
T-6a	–	–	–
T-7a	53.8	54.3	0.5
T-8a	–	–	–
TWG-1	57.4	60.4	3.0
TWG-2	55.9	58.8	2.9
TWG-3	55.0	57.2	2.2
TWG-4	54.4	57.3	2.9
TWG-5	<54.8	56.3	>1.5
TWG-6	<55.5	58.0	>2.5
TWG-7	59.7*	61.2*	1.5*
	<57.7	59.7	>2.0
T-1b	<59.0	60.2	>1.2
T-2b	<57.2	58.9	>1.7
T-3b	<60.2	62.7	>2.5
T-4b	<57.2	58.7	>1.5
T-5b	<56.5	57.8	>1.3
T-6b	<56.4	57.4	>1.0

*Concerns the clay layer within the crevasse-splay complex.

Description of the studied sections

The vertical sections I–III of the sandy complex are located along the western exploitation wall of the Tomisławice opencast (Figs 1B, 4). The sections are spaced at ~50 m along a straight-line mining wall, with geographic co-ordinates from 52°28′11.5′′N to 18°30′48.3′′E. These sections include both the interseam sands with lignite interbeds and the lower and upper benches of the MPLS-1 with a clay interlayer. The sandy complex, together with lignite intercalations, has a thickness ranging from 4.3 to 4.8 m (Figs 4B–D, 7).

In the vicinity of the examined sections, the sand bodies are underlain by the main, lower lignite bench, which is 4.9–5.1 m thick. The upper lignite bench, overlying the sand bodies, is only ~1.5 m thick (Fig. 7). This bench contains a thin (up to 30 cm) interlayer of clay. The sand bodies of the complex are separated by three layers of lignite, with a total thickness of 1–1.2 m in all three sections. It should be noted that only two sand bodies were identified in the boreholes, mainly owing to wet drilling, while detailed field studies (sections I–III) allowed recognition of as many as four sandy units (see Figs 5, 7). This discrepancy also could be due to the amalgamation of sand bodies (van Toorenenburg *et al*., 2016; Burns *et al*., 2019; Colombera and Mountney, 2021; Rahman *et al*., 2022a, b; and other references therein).

Facies associations

In this paper, the siliciclastic sediments are divided into two main facies groups, on the basis of their textural and structural characteristics. They are categorized as subaerial and subaqueous facies associations and are described and interpreted in this order below. In general, the first facies association is represented by the deposits of the two middle sand bodies, while the second facies association includes deposits of the lowest and highest sand bodies (Fig. 7).

Subaerial facies

Description: This set of facies forms the subaerial sand bodies but contributes also to the subaqueous ones in the sections studied. The subaerial association comprises the following sandy-coaly and sandy facies: SCh, Sh, SCm, and Sm (Figs 7B, 8; Tab. 2). Sands and coaly sands with massive structure (facies SCm and Sm) predominate. The sands are well to very well sorted and fine-grained, with grain sizes ranging from 0.13 to 0.19 mm (average 0.15 mm). No vertical grading of grain-size fractions was recognized in the massive sand beds.

Most of these facies contain concentrations of plant detritus (0.2–3.7 wt.%, average 1.6 wt.%), as well as the roots of bushy or woody vegetation. The facies are thus coaly (carbonaceous) and are characterized by massive structure or planar horizontal stratification (Figs 7B, 8). Small amounts (<1 wt.%) of organic matter were found in samples T12–T16 and T19–T22 (Fig. 8).

Interpretation: The horizontally stratified coaly sands and sands (facies SCh, Sh; Tab. 2) can be interpreted as deposited

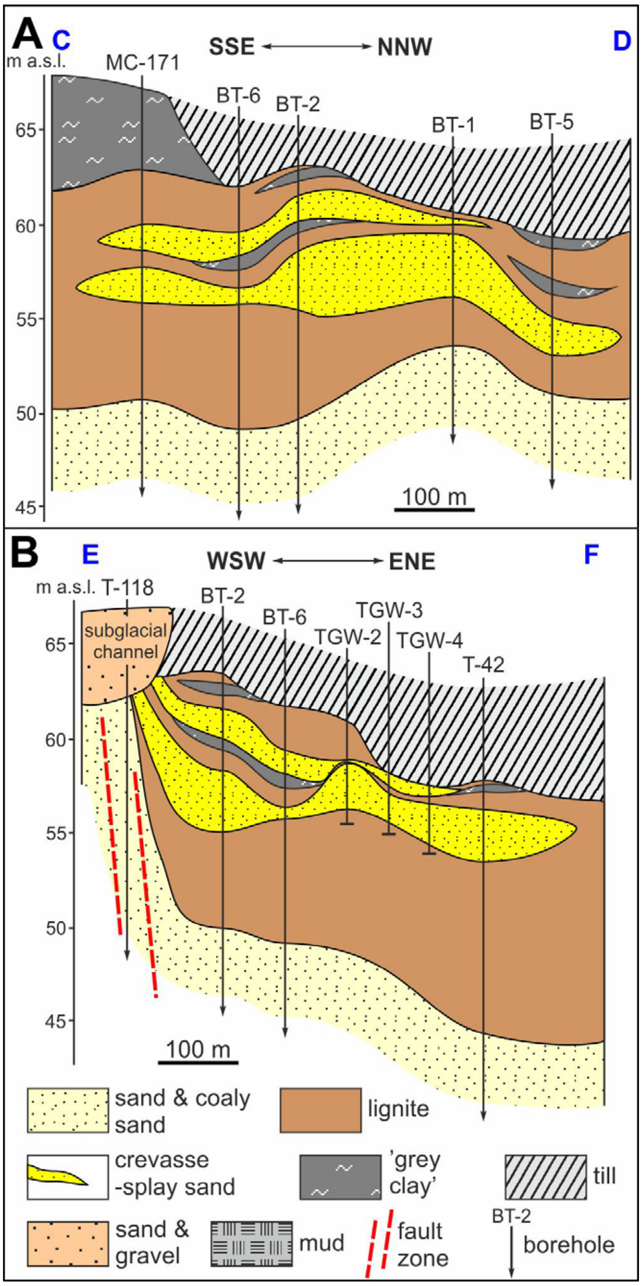

Fig. 5. Geological cross-sections through the sand bodies within the MPLS-1. **A.** The cross-section C–D with upwardly convex sandy sediments. **B.** The cross-section E–F with sandy sediments, generally dipping to the east. For the location of both cross-sectional lines, see Figure 1B.

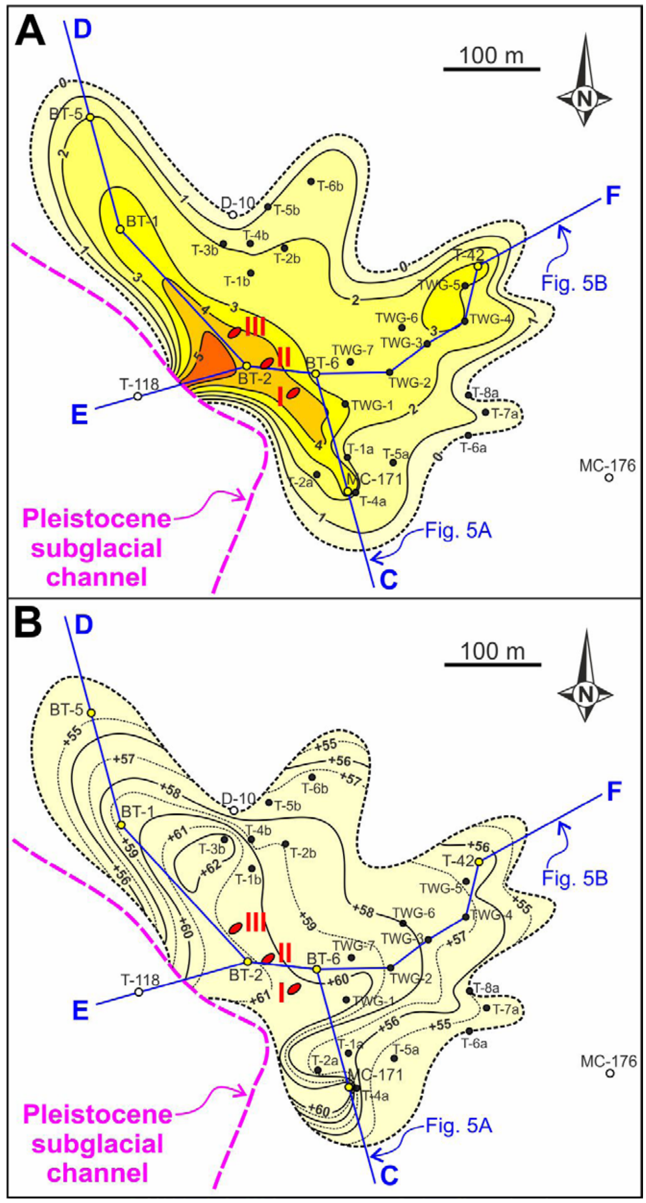

Fig. 6. Sandy complex shown in plan view. **A.** Thickness map of the interseam sands with isopachs every 1 m. **B.** Structural map of the complex top with structure contours in m a.s.l. For borehole data, see Table 1; note the location of the geological cross-sections C–D and E–F, and sections I–III, examined in detail.

over the entire surface of the successive crevasse-splays. The water spread as a sheet flow during the formation of these facies, with sand transported as an upper-stage plane bed (McKee *et al.*, 1967; Gradziński *et al.*, 1976; Miall, 1977; Allen, 1982, 1984; Bridge, 2003; Zieliński, 2014; and other references therein). The attribution of massive sands (facies SCm, Sm) to rapid dumping from a hyperconcentrated flow (e.g., Pierson, 2005; Nemec, 2009) may seem misleading and hence needs to be clarified briefly.

Only traces of small-scale cross-stratification structures were found within the dominantly massive sands in the present case (see Appendix). However, such structures are known from the massive sands of a crevasse splay in the southern segment of the Tomisławice opencast (Widera, 2016a; Widera *et al.*, 2017a; Chomiak, 2020). These massive sands thus involved at least transient tractional deposition, with the migration of ripples and small dunes. The lack of stratification in the massive sands could be due to their good sorting and/or pedogenic processes. The bioturbation, caused by the roots of peat-forming vegetation, may have obscured, disturbed or destroyed the original stratification (e.g., Miall, 2006; Boggs, 2012; Gulliford *et al.*, 2014).

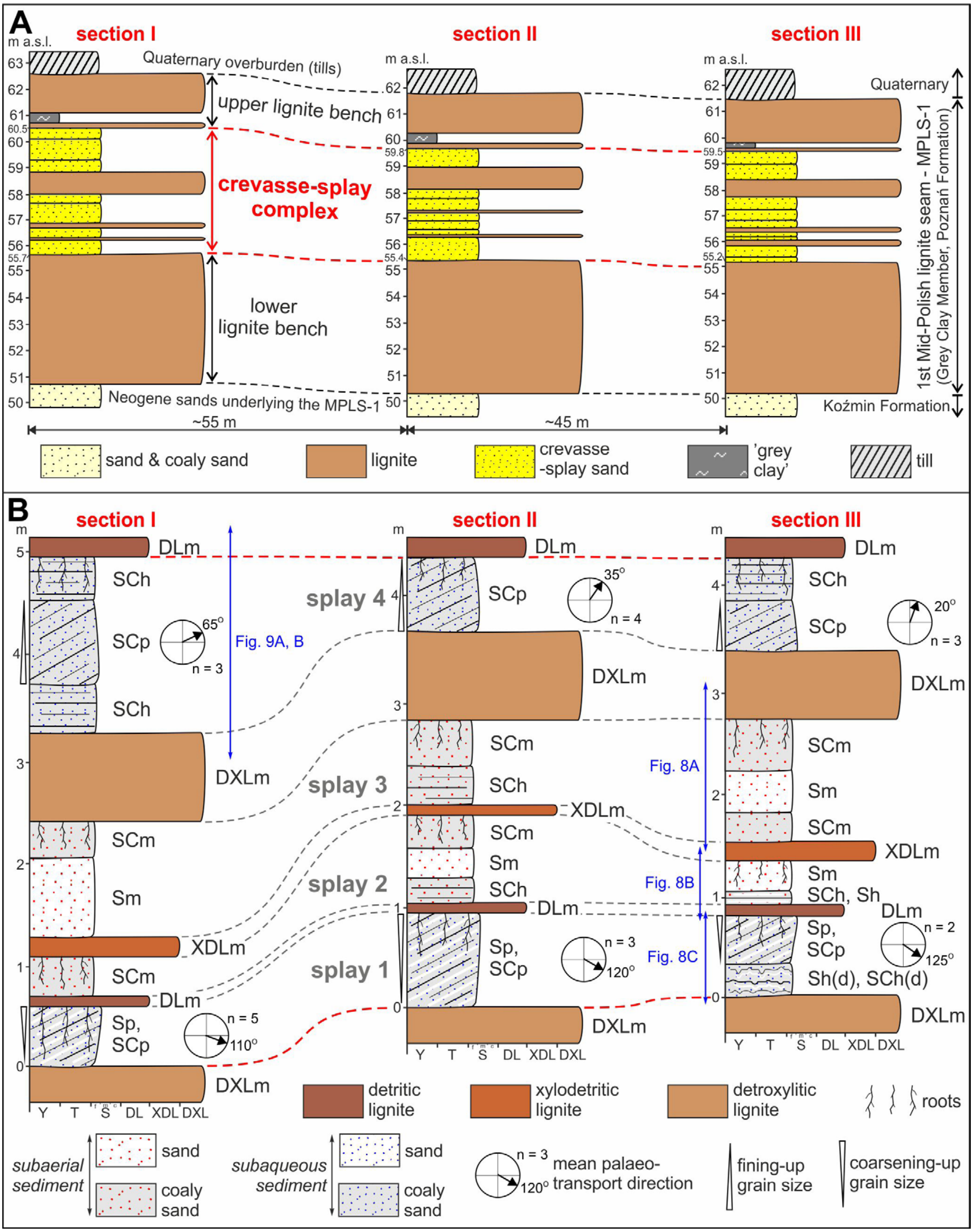

Fig. 7. Representative sections of the sandy sediments in the Tomisławice lignite opencast. **A.** General view of the sand bodies within the MPLS-1. **B.** Sedimentary logs of sections I–III, analyzed in detail. For their locations, see Figures 1B, 6; for an explanation of facies and lithotypes codes, see Table 2.

Table 2

Codification of sandy facies (Miall, 1977) and lignite lithotypes (Widera, 2012, 2016b), used in this paper. *Facies codes used in the Appendix only.

Sand facies	
Code	Description
Sm	sand with massive structure
SCm	coaly (carbonaceous) sand with massive structure
Sh	horizontally laminated sand
Sh(d)	deformed horizontally laminated sand
SCh	horizontally laminated coaly (carbonaceous) sand
SCh(d)	deformed horizontally laminated coaly sand
Sp	sand with planar cross-stratification
SCp	coaly sand with planar cross-stratification
St*	trough cross-stratified sand
SCt*	trough cross-stratified coaly (carbonaceous) sand
Sr*	ripple cross-laminated sand
Lignite lithotypes	
DLm	detritic lignite with massive structure
XDLm	xylodetritic lignite with massive structure
DXLm	detroxylitic lignite with massive structure

Subaqueous facies

Description: Planar cross-stratified sands and coaly sands (facies Sp, SCp; Tab. 2) occur within the lowest and highest splay sand bodies, where they persist at two levels over a distance of >200 m, including the studied sections (Figs 7B, 8C, 9). Both levels involve fine-grained sand with grain sizes ranging from 0.14 to 0.17 mm (average 0.16 mm). The stratification is inclined at angles of 10–35° towards the ESE (mean resultant azimuth in the range of 110–125°) at the lower level, and towards the NNE (mean azimuth in the range of 20–65°) at the upper level. The bulk thickness of facies SCp and Sp at each level is between 30 and 90 cm (Fig. 7B).

The lower level of facies SCp and Sp is characterized by slight upwards coarsening (from 0.14 to 0.15 mm; samples T5–T8), whereas the opposite is the case at the upper level, where the grain size is fining upwards (from 0.17 to 0.15 mm; samples T26–T29 and T30–T34; Dziamara *et al*., 2023). It is also worth noting that the SCh(d) and Sh(d) facies in section III seem to be related genetically to the overlying facies Sp and SCp (Figs 7B, 8C; Table 2). Soft-sediment deformation includes, among other types, load casts, ball-and-pillow structures, and flame structures up to 3–5 cm high (Fig. 8C).

Interpretation: Facies SCp and Sp differ only in their organic matter content, with their textural and structural features the same, which allows the grouping of them as one facies set. Owing to their planar cross-stratification, large lateral spread (>200 m), and their similar dip angles (up to 35°), and direction of lamination dip (~115° and ~30°, respectively), these facies should be considered as the

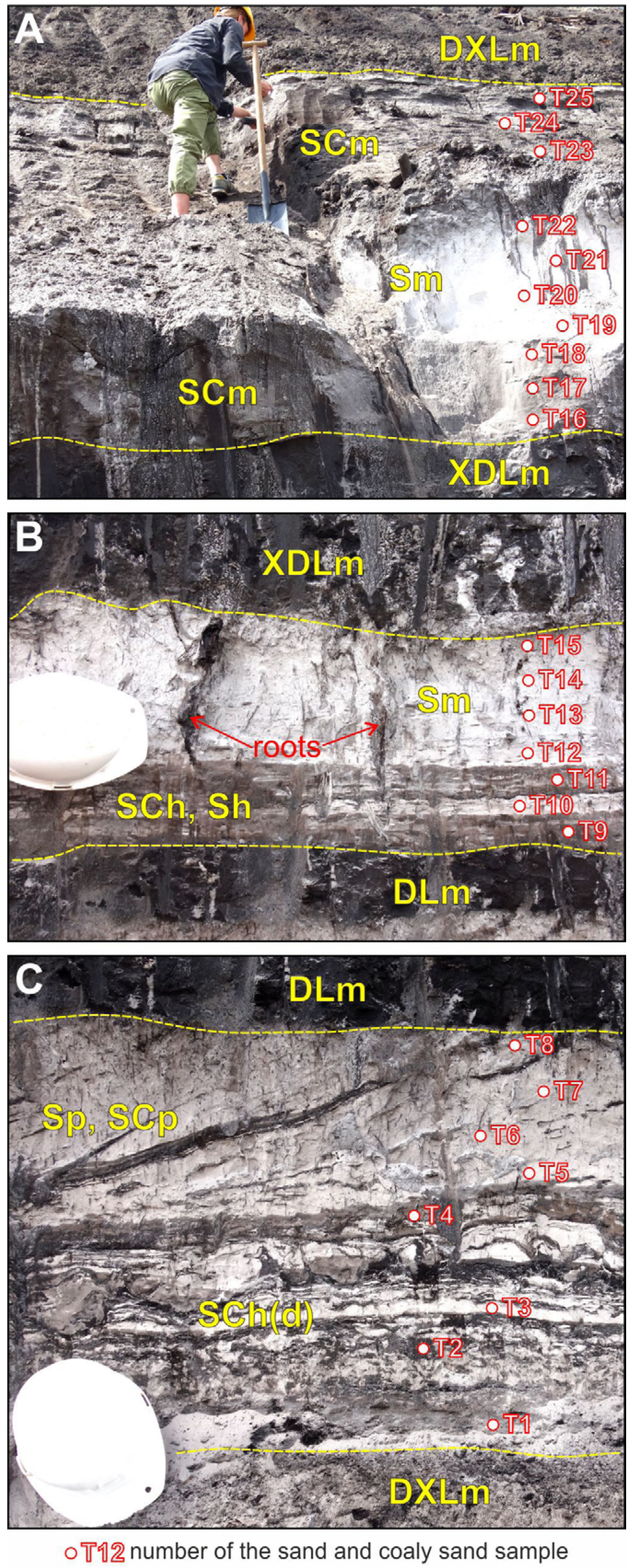

Fig. 8 Examples of the sandy facies and accompanying lignite lithotypes in section III. Note the locations of the samples analyzed for grain size and organic content; for the location of the photos, see Figure 7B; for an explanation of facies and lithotypes codes, see Table 2.

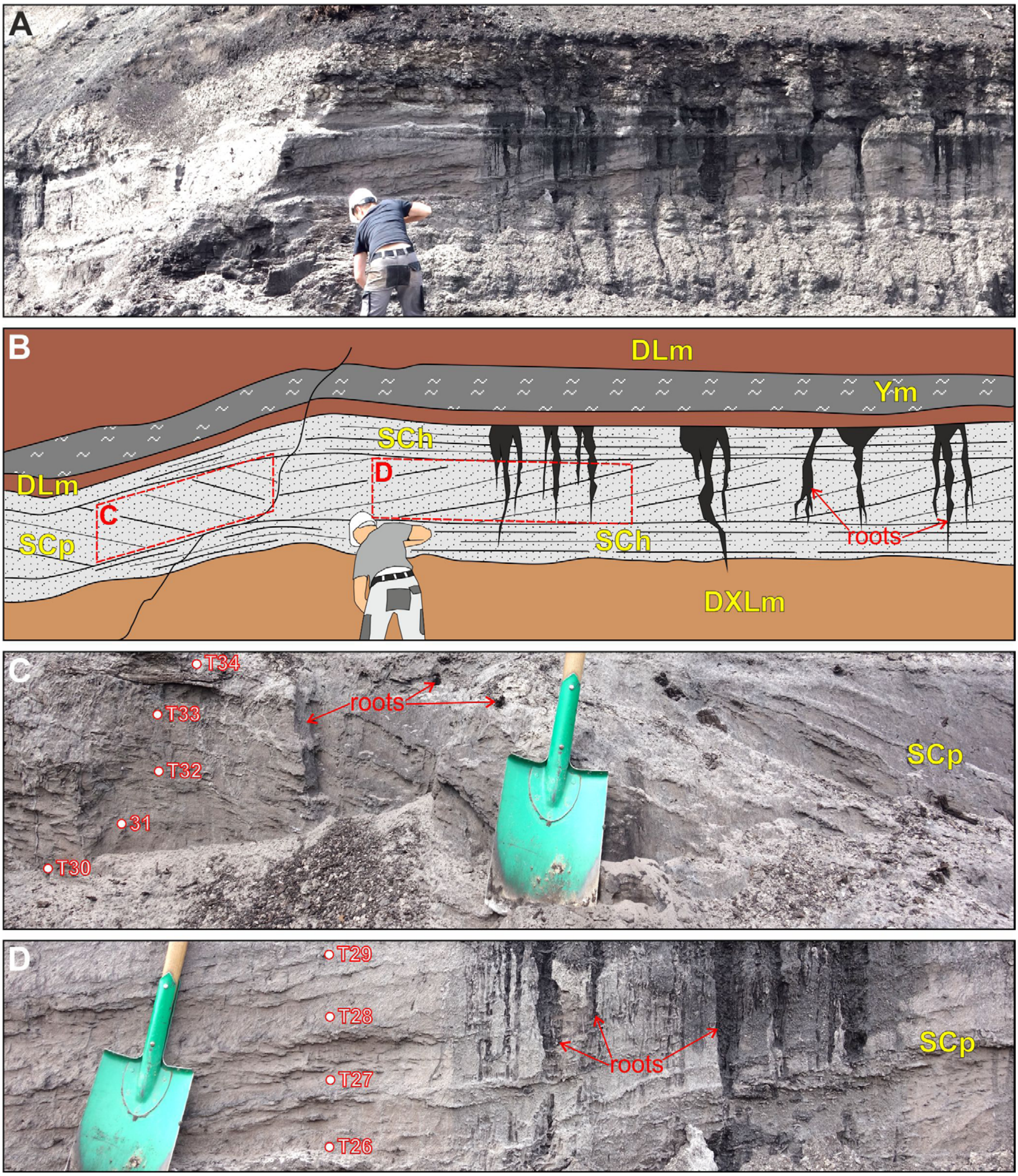

Fig. 9. Planar cross-stratified coaly sand, typical of the crevasse-splay microdelta in section I. **A.** Broad view of the microdelta sediments. **B.** Corresponding line-drawing for Figure 9A. **C, D.** Detailed view of the microdelta sediments, marked in Figure 9B. Note the location of the samples analyzed for grain size and organic content; for the location of the photos, see Figure 7B; for an explanation of facies and lithotypes codes, see Table 2.

rock record of two crevasse splays of similar genesis (cf. Figs 7B, 8C, 9). In other words, the interpreted facies (SCp, Sp) are typical of the delta's 'prograding splay deposits' (e.g., Bristow *et al.*, 1999; Michaelsen *et al.*, 2000; Zieliński, 2014), accumulated in shallow lakes or ponds that certainly existed (see the interpretation of lignite lithotypes below) on the surface of the mid-Miocene mire in the study area (Widera, 2016a, b, 2022; Widera *et al.*, 2017a; Chomiak *et al.*, 2020; Dziamara *et al.*, 2022, 2023). Considering their small size (<<1 km^2) and genetic relationship with the crevasse splays, the depositional forms represented by the SCp and Sp facies can be termed subdeltas (Mjøs *et al*., 1993), lacustrine (micro)deltas (Tye and Coleman, 1989; Morozova and Smith, 2000; Rajchl and Uličny, 2005; Rajchl *et al*., 2008; Davies-Vollum *et al*., 2012; Wang *et al*., 2020), crevasse deltas (Gradziński *et al*., 2005; Kędzior *et al*., 2007; Jerrett *et al*., 2016), crevasses with deltas (Lewin *et al*., 2017), or crevasse-splay microdeltas (Teisseyre, 1985; Zwoliński, 1985, 1992; Zieliński, 2014; Chomiak *et al*., 2019; Wachocki *et al*., 2020; Widera *et al*., 2022, 2023; and other references therein).

The slight coarsening-upwards and fining-upwards of grain sizes in the lower and upper microdelta deposits, respectively, may have several causes. The first case may take place during an increase in water-flow energy, resulting in a prograding crevasse splay (Fielding, 1984), with the supply of increasingly coarser grains from the crevasse channel being a result of the natural levee erosion (Gębica and Sokołowski, 2001) or the progradation of the splay into the lake or pond (Davies-Vollum *et al*., 2012). On the other hand, the fining-upwards trend is believed to be more common in crevasse-splay sediments and is interpreted as recording a weakening of water-flow energy (e.g., Jorgensen and Fielding, 1996; Farrell, 2001; Burns *et al*., 2017; Widera *et al*., 2023). However, both trends (upwards-fining and -coarsening) are also possible, i.e., prograding and retrograding crevasse-splay microdeltas (e.g., Bristow *et al*., 1999; Makaske, 2001; Mach *et al*., 2013; Jerrett *et al*., 2016; Wang *et al*., 2020).

The complete delta sequence, including the crevasse-splay microdelta, consists of three parts, namely the topset, foreset, and bottomset, corresponding to the delta plain, delta front, and prodelta, respectively (e.g., Gradziński *et al*., 1976; Easterbrook, 1999; Rajchl and Uličny, 2005; Boggs, 2012; Zieliński, 2014; and other references therein). The topset layers perhaps are only those that are horizontally stratified and lie above the interpreted SCp and Sp facies, the upper microdelta sediments in sections I and III (Figs 7B, 9A, B). The planar cross-stratified coaly sands and sands (SCp, Sp) represent the foreset beds. Only the SCh(d) facies can be considered to represent the bottomset layers with certainty. This is the only observed case, where all sets of facies (SCh(d), Sh(d), and SCp, Sp) continue to form large-scale tangential cross-stratification together (Fig. 8C; Tab. 2). On the other hand, the small-scale soft-sediment deformations of the bottomset laminae can be interpreted as a result of reversed density gradients or unequal loading (e.g., Anketell and Dżułyński, 1968; Allen, 1982; Chomiak *et al*., 2019). In this case, they were most likely produced syn-depositionally by ripples, migrating on liquefied, heterolithic deposits (sands *vs* coaly sands; see Fig. 8C), and therefore an unstable substrate (Anketell *et al*., 1970; and other papers of these authors).

Lignite lithotype association

Description: The lignite lithotypes that are positioned above and below, as well as within the crevasse-splay complex, are as follows: DLm – detritic lignite with a massive structure, XDLm – xylodetritic lignite with a massive structure, and DXLm – detroxylitic lignite with a massive structure.

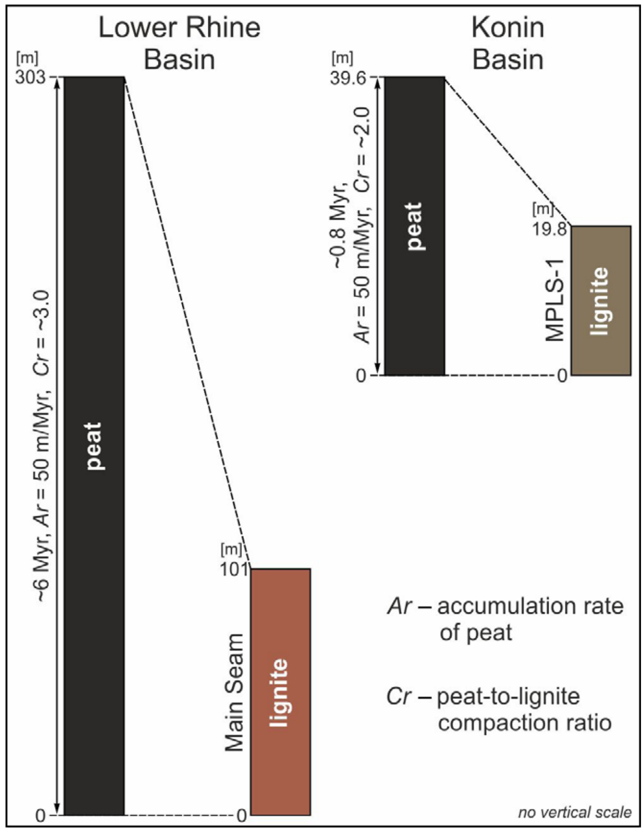

Fig. 10. Simplified sketch, showing the method of estimating the accumulation time of the MPLS-1 in the Konin Basin by comparison with the Main Seam in the Lower Rhine Basin (data obtained from Hager *et al*., 1981; Zagwijn and Hager, 1987; Piwocki, 1992; Widera *et al*., 2007, 2021a; Widera, 2013, 2015; Chomiak, 2020). Note that the assumed accumulation rate of peat (*Ar*) is the same, while the peat-to-lignite compaction ratios (*Cr*) are different in both cases; for other explanations, see the text.

The same lithotypes also separate the sand bodies, although the thickest layer of lignite (DXLm) occurs in all sections that were studied in detail, where it has a thickness of 0.6–0.9 m. The thickness of the thinner lignite beds (XDLm, DLm) ranges from 0.1 to 0.4 m (Figs 7B, 8, 9A, B; Tab. 2).

The detroxylitic lignite with a massive structure (DXLm) contains paradoxically more xylites (i.e., fossilized wood remains >1 cm in size) than detrital matrix (i.e., fine-graded plant detritus <1 cm in size). In xylodetritic lignite with a massive structure (XDLm), on the other hand, the opposite is true and xylites predominate over plant detritus. However, over 90% of the detritic lignite consists of a detrital matrix, while up to 10 vol.% may consist of xylites, other lithotypes or mineral admixtures – the so-called '10% rule' (cf. Kwiecińska and Wagner, 1997; Markič and Sachsenhofer, 1997; Ticleanu *et al*., 1999; Widera, 2012, 2016b, 2021, 2022; and other references therein).

Interpretation: The DXLm is typical of wet-forest swamp depositional environments, which are known as *Taxodium–Nyssa* swamps (Teichmüller, 1958; 1989). The occurrence of such hydrophilic trees in this lithotype (e.g., Słodkowska and Widera, 2021, 2022; Worobiec *et al*., 2021, 2022) may indicate that the water table was relatively high, above the depositional surface. The water table was slightly lower at the time of XDLm formation. Then, bushy peat-forming vegetation dominated, creating a Myricaceae-Cyrillaceae swamp (Teichmüller, 1958, 1989).

The environment of DLm deposition seems to be of particular importance within the association of lignite lithotypes. It is interpreted as having occurred within a fen or open water, that is, a lake or pond, existing in the mire area. Teichmüller (1958, 1989) compared this type of mire to modern treeless reed marshes, dominated by herbaceous vegetation, such as reeds, sedges, ferns, and aquatic plants (Kwiecińska and Wagner, 1997; Markič and Sachsenhofer, 1997; Ticleanu *et al*., 1999; Mach *et al*., 2013; and other references therein). Thus, a large part of the peat, which then transformed into detritic lignite (DLm), was accumulated in shallow lakes/ponds that were usually <2 m deep (e.g., Flores, 1981; Tye and Coleman, 1989; Diessel *et al*., 2000; Bos *et al*., 2009; Chomiak *et al*., 2020; Widera *et al*., 2021a). This value is the mean maximum water depth for rooted aquatic vegetation (especially *Nuphar*, *Nymphaea*, *Potamogeton*, *Myriophyllum*, *Ceratophyllum*, etc.) in the littoral zone of the lake/pond (e.g., Kłosowski *et al*., 2011). This is true for both modern and ancient shallow-water environments. Thus, the above statement further supports the view that water stagnated on the surface of the mid-Miocene mires in central Poland and that the crevasse-splay sediments subsequently were deposited on these as microdeltas.

Accumulation time of the crevasse-splay complex

It is commonly accepted that the time of deposition of a crevasse-splay element lasts from a few days to several years (e.g., Kraus and Wells, 1999; Lepre, 2017). The interval given is negligible in relation to the formation time of lignite seams worldwide. For example, the accumulation of the youngest, world-famous Quaternary lignite in the Philippi peatland (Greece) must have occurred over <700 kyr (cf. Christianis *et al*., 1998 and Widera, 2021), while the Main Seam in the Lower Rhine Basin (Germany) was built up over ~6 Myr (Zagwijn and Hager, 1987). Owing to the lack of other methods for calculating the formation time of the crevasse-splay complex studied in this paper, the former will be estimated indirectly by determining the accumulation time of three lignite beds, separating the successive splays (see Figs 4, 5, 7, 8). To this end, it can be assumed that the total age of these lignites (1.2 m thick in section I; Fig. 7B) approximates the age of the entire sand-body complex, including hiatuses in crevasse-splay deposition.

As mentioned above, the Main Seam (Lower Rhine Basin, Germany), with a maximum thickness of 101 m, was formed in ~6 Myr (Zagwijn and Hager, 1987). This means that 1 m of this seam would have been formed during over ~60 kyr. It is worth adding that the maximum thickness of the First Mid-Polish Lignite Seam (MPLS-1; Konin Basin, Poland) is only 19.8 m (Piwocki, 1992; Widera, 2013b). It should be assumed here that the rate of peat accumulation was the same, while the deposition time of 1 m of both seams was not the same, since they had different peat-to-lignite compaction ratios (Fig. 10). They were ~3.0 for the Lower Rhine lignites and ~2.0 for the Konin lignites (cf. Hager *et al*., 1981; Widera *et al*., 2007; Widera, 2015; and other references therein). Simple calculations showed that 1 m of the MPLS-1 had been deposited by ~40 ka (Chomiak, 2020; Widera *et al*., 2021a), while 1.2 m of lignite (three thin layers in total) was generated over 48 kyr. Thus, at the current stage of research, it can be concluded that the crevasse-splay complex studied could have accumulated during >48 kyr.

DISCUSSION

Environmental conditions of the crevasse-splay complex formation

The First Mid-Miocene Lignite Seam (MPLS-1), containing the investigated crevasse-splay complex, was deposited during ~15.1–14.3 Ma. This means that its formation began at the time of the last peak of the Mid-Miocene Climate Optimum and continued relatively shortly after it (Widera *et al*., 2021a, b). On the basis of recent palynological analyses from the Konin Basin, it was determined that the mean annual temperature at the time was within the range of 15.7–20.5 °C, and the mean annual precipitation from 1,300 mm to 1,500 mm. Therefore, it can be concluded that the climate was warm-temperate and humid with progressive cooling, drying, and seasonality during accumulation of the MPLS-1 (Słodkowska and Widera, 2021, 2022; Worobiec *et al*., 2021, 2022). This trend also is confirmed by geochemical studies of the same lignite seam in the study area (Bechtel *et al*., 2019, 2020).

The aforementioned progressive seasonality of the climate at the time of formation of the MPLS-1 resulted, among other conditions, in periodically increased precipitation, which led to floods. This is confirmed by the crevasse-splay sediments studied, but also by the clay layers within the lignite seam (see Figs 7A, 9A, B; Chomiak *et al*., 2020). Obviously, the floods came from the nearby channels of rivers that flowed around the mid-Miocene low-lying mires. This statement is confirmed by the occurrence of sandy sediments of numerous crevasse splays, which were accumulated in almost opposite directions, i.e., towards the axial zone of the current 'Tomisławice' lignite deposit (Chomiak *et al*., 2020). Therefore, the mire, from which this lignite deposit was created, can be called a backswamp (e.g., Flores, 1981; Flores and Hanley, 1984; McCabe, 1984; Diessel *et al*., 2000; Davies-Vollum and Kraus, 2001; Chomiak *et al*., 2019; and other references therein).

Uniqueness of the crevasse-splay complex

Exposures of crevasse-splay deposits in the rock record are rare in relation to modern sedimentary environments, especially those found in hard coal or lignite successions. The exceptions are the crevasse splays, known from the Konin Basin in central Poland. This is due to the fact that in recent years, more marginal parts of the deposits have been exploited (even selectively), where the lignite seams are thinner and often interbedded with sands (Widera *et al*., 2022). So far, in the Tomisławice and Pątnów IIB opencasts, managed by the Konin Lignite Mine, sediments of at least six crevasse splays have been described, where in two cases these splays were superposed (Widera, 2016a, 2020; Widera *et al*., 2017a, 2023; Chomiak *et al*., 2019; Chomiak, 2020; Wachocki *et al*., 2020; Dziamara *et al.*, 2022, 2023). They represent subaerial and subaqueous types, as well as deformed and undeformed subtypes of crevasse splays (Widera *et al.*, 2023).

To the best of the knowledge of the present authors, the complex studied in this paper (up to 4.8 m thick in the field and 6.5 m thick in boreholes) is one of the best developed, as described in Polish and world literature. First, it consists of four (locally five, as documented during supplementary studies in August and September 2022) superposed splay elements. Second, the deposition of these splays most likely resulted from various crevasse channels cutting the natural levee. Third, the deposition took place at least twice in a shallow lake or pond, located on the surface of the mid-Miocene backswamp. And fourth, for the first time in the history of the Konin Lignite Mine, the upper lignite bench and the sands of the crevasse-splay complex were exploited selectively. Ultimately, the lignite was sent to the power plant for the production of electricity, while the sands were deposited on the internal dumps of the Tomisławice opencast.

CONCLUSIONS

A sandy complex at the Tomisławice lignite opencast (central Poland) comprises four splay horizons in vertical sequence, which are separated by thin (0.1–0.8 m) layers of lignite. This has been observed only quite rarely in the rock record, especially in natural and man-made exposures. Hence, the available borehole data and direct field observations allowed the authors to carry out a detailed sedimentological analysis of the complex studied.

The sediments are mainly fine-grained, coaly sands and only occasionally comprise sands without any admixture of other fractions and organic matter. These generally sandy deposits were identified within the First Mid-Polish Lignite Seam (MPLS-1) and were accumulated in subaerial and subaqueous conditions, as indicated by their characteristic structural features. In the first case, they are horizontally stratified sands (SCh, Sh facies), which are typical for sheet flows, but massive sands (SCm, Sm facies) predominate and are interpreted as the result of strong bioturbation of the sediments by the roots of peat-forming vegetation.

The second case is characterized by two well-developed and widely spread planar cross-stratification sets (SCp, Sp) and also locally by facies SCh, Sh(d) and SCh(d). Their lamination is steeply dipping (up to 35°) in different directions (115°, 30°) and is recognized as representing the prograding splay deposits that are typical of deltas. These sediments were combined with two crevasse-splay microdeltas that were formed in shallow lakes/ponds, existing on the surface of a mid-Miocene backswamp.

Calculations, based on the estimated age of the lignite interbeds (a total of 1.2 m in thickness), revealed that the complex studied could have been created over 48 kyr. On the other hand, the presence of four superposed splay elements, representing the records of successive floods, is proof of the increasing seasonality, which followed the last peak of the mid-Miocene Climate Optimum. The sandy crevasse-splay complex, investigated in this paper, is the best developed, so far identified in the entire lignite-bearing Miocene of Poland.

Acknowledgements

The study was funded by the Adam Mickiewicz University in Poznań, Poland. The authors wish to thank S. Leszczyński (Jagiellonian University, Kraków, Poland) and R. M. Jerrett (University of Manchester, United Kingdom) for insightful reviews, as well as W. Nemec (University of Bergen, Norway) and M. Gradziński (Jagiellonian University, Kraków, Poland) for editorial work.

REFERENCES

Allen, J. R. L., 1982. *Sedimentary Structures: Their Character and Physical Basis*. *Vol. II*. Elsevier, New York, 663 pp.

Allen, J. R. L., 1984. Parallel lamination developed from upper-stage plane beds: a model based on the larger coherent structures of the turbulent boundary layer. *Sedimentary Geology*, 39: 227–242.

Anketell, J. M., Cegła, J. & Dżułyński, S., 1970. On the deformational structures in systems with reversed gravity gradient. *Rocznik Polskiego Towarzystwa Geologicznego*, 40: 3–29.

Anketell, J. M. & Dżułyński, S., 1968. Patterns of density controlled convolutions involving statistically homogeneous and heterogeneous layers. *Rocznik Polskiego Towarzystwa Geologicznego*, 38: 401–409.

Baeteman, C., Beets, D. J. & Van Strydonck, M., 1999. Tidal crevasse splays as the cause of rapid changes in the rate of aggradation in the Holocene tidal deposits of the Belgian Coastal Plain. *Quaternary International*, 56: 3–13.

Bechtel, A., Widera, M., Lücke, A., Groß, D. & Woszczyk, M., 2020. Petrological and geochemical characteristics of xylites from the First Lusatian lignite seam (Konin Basin, Poland): implications for floral sources, decomposition and environmental conditions. *Organic Geochemistry*, 147: 104052.

Bechtel, A., Widera, M. & Woszczyk, M., 2019. Composition of lipids from the First Lusatian lignite seam of the Konin Basin (Poland): relationships with vegetation, climate and carbon cycling during the mid-Miocene Climatic Optimum. *Organic Geochemistry*, 138: 103908.

Boggs, S., 2012. *Principles of Sedimentation and Stratigraphy*. New Jersey, Prentice Hall, 218 pp.

Bos, I. J., Busschers, F. S. & Hoek, W. Z., 2012. Organic-facies determination: a key for understanding facies distribution in the basal peat layer of the Holocene Rhine–Meuse delta, The Netherlands. *Sedimentology*, 59: 679–703.

Bos, I. J., Feiken, H., Bunnik, F. & Schokker, J., 2009. Influence of organics and clastic lake fills on distributary channel processes in the distal Rhine-Meuse delta (The Netherlands). *Palaeogeography, Palaeoclimatology, Palaeoecology*, 284: 355–374.

Bridge, J., 2003. *Rivers and Floodplains – Forms, Processes and Sedimentary Record*. Blackwell Science, Oxford, 491 pp.

Bristow, C. S., Skelly, R. L. & Ethridge, F. G., 1999. Crevasse splays from the rapidly aggrading, sand-bed, braided Niobrara River, Nebraska: effect of base-level rise. *Sedimentology*, 46: 1029–1048.

Brzyski, B., Gradziński, R. & Krzanowska, R., 1976. Standing trunks of calamites in the exposure Brynów brickyard and conditions for their burial. *Rocznik Polskiego Towarzystwa Geologicznego*, 46: 159–182. [In Polish, with English summary.]

Burns, C. E., Mountney, N. P., Hodgson, D. M. & Colombera, L., 2017. Anatomy and dimensions of fluvial crevasse-splay deposits: examples from the Cretaceous Castlegate Sandstone and Neslen Formation, Utah, USA. *Sedimentary Geology*, 351: 21–35.

Burns, C. E., Mountney, N. P., Hodgson, D. M. & Colombera, L., 2019. Stratigraphic architecture and hierarchy of fluvial overbank splay deposits. *Journal of Geological Society,* 176: 629–649.

Cahoon, D. R., White, D. A. & Lynch, J. C., 2011. Sediment infilling and wetland formation dynamics in an active crevasse splay of the Mississippi River delta. *Geomorphology*, 131: 57–68.

Chakraborty, T., Kar, P., Ghosh, P. & Basu, S., 2010. Kosi Megafan: Historical records, geomorphology and the recent avulsion of the Kosi River. *Quaternary International*, 22: 143–160.

Chomiak, L., 2020. Crevasse splays within a lignite seam at the Tomisławice opencast mine near Konin, central Poland: architecture, sedimentology and depositional model. *Geologos*, 26: 25–37.

Chomiak, L., Maciaszek, P., Wachocki, R., Widera, M. & Zieliński, T., 2019. Seismically-induced soft-sediment deformation in crevasse-splay microdelta deposits (Middle Miocene, central Poland). *Geological Quarterly*, 63: 162–177.

Chomiak, L., Urbański, P. & Widera, M., 2020. Geological record of the lacustrine stage in the evolution of the Mid-Miocene mire – the Tomisławice lignite opencast near Konin in central Poland. *Przegląd Geologiczny*, 68: 526–534. [In Polish, with English abstract.]

Christanis, K., Georgakopoulos, A., Fernández-Turiel, J. L. & Bouzinos, A., 1998. Geological factors influencing the concentration of trace elements in the Philippi peatland, eastern Macedonia, Greece. *International Journal of Coal Geology*, 36: 295–313.

Cloyd, K. C., Demicco, R. V. & Spencer, R. J., 1990. Tidal channel, levee, and crevasse-splay deposits from a Cambrian tidal channel system: a new mechanism to produce shallowing-upward sequences. *Journal of Sedimentary Petrology*, 60: 73–83.

Colombera, L. & Mountney, N. P., 2021. Influence of fluvial crevasse-splay deposits on sandbody connectivity: Lessons from geological analogues and stochastic modelling. *Marine and Petroleum Geology*, 128: 105060.

Dadlez, R., Marek, S. & Pokorski, J. (eds), 2000. *Mapa Geologiczna Polski bez kenozoiku w skali 1:1000000*. Państwowy Instytut Geologiczny, Warszawa. [In Polish.]

Davies-Vollum, K. S., Guion, P. D., Satterfield, D. A. & Suthren, R. J., 2012. Lacustrine delta deposits and their effects on coal mining in a surface mine in Derbyshire, England. *International Journal of Coal Geology*, 102: 52–74.

Davies-Vollum, K. S. & Kraus, M. J., 2001. A relationship between alluvial backswamps and avulsion cycles: an example from the Willwood Formation of the Bighorn Basin, Wyoming. *Sedimentary Geology*, 140: 235–249.

Diessel, C., Boyd, R., Wadsworth, J., Leckie, D. & Chalmers, G., 2000. On balanced and unbalanced accommodation/peat accumulations ratios in the Cretaceous coals from Gates Formation, Western Canada, and their sequence-stratigraphic significance. *International Journal of Coal Geology*, 43: 143–186.

Doktor, M., 2007. Conditions of accumulation and sedimentary architecture of the upper Westphalian Cracow Sandstone Series (Upper Silesia Coal Basin, Poland). *Annales Societatis Geologorum Poloniae*, 77: 219–268.

Dziamara, M., Glacová, V., Klęsk, J., Marschalko, M., Wachocki, R. & Widera, M., 2022. The impact of sandy interbeddings in lignite on mining activities – an example from the "Pątnów" IV deposit (Konin vicinity) in central Poland. *Przegląd Geologiczny*, 70: 376–383. [In Polish, with English abstract.]

Dziamara, M., Kaczmarek, P., Klęsk, J., Wachocki, R. & Widera, M., 2023. Facies and statistical analyses of a crevasse-splay complex at the Tomisławice opencast lignite mine in central Poland. *Geologos*, 29: 173–181.

Easterbrook, D. J., 1999. *Surface Processes and Landforms*. New Jersey, Prentice Hall, pp. 352.

Farrell, K. M., 2001. Geomorphology, facies architecture, and high-resolution, non-marine sequence stratigraphy in avulsion deposits, Cumberland Marshes, Saskatchewan. *Sedimentary Geology*, 139: 93–150.

Fielding, C. R., 1984. Upper delta plain lacustrine and fluviolacustrine facies from the Westphalian of the Durham coalfield, NE England. *Sedimentology*, 31: 547–567.

Fisher, J. A., Krapf, C. B. E., Lang, S. C., Nichols, G. J. & Payenberg, T. H. D., 2008. Sedimentology and architecture of the Douglas Creek terminal splay, Lake Eyre, central Australia. *Sedimentology*, 55: 1915–1930.

Flores, R. M., 1981. Coal deposition in fluvial palaeoenvironments of the Palaeocene Tongue River Member of the Fort Union Formation, Powder River area, Powder River Basin, Wyoming and Montana. In: Ethridge, F. G. & Flores, R. M. (eds), *Nonmarine Depositional Environments: Models for Exploration. Society of Economic Paleontologists and Mineralogists, Special Publication*, 31: 169–190.

Flores, R. M. & Hanley, J. H., 1984. Anastomosed and associated coal-bearing fluvial deposits: Upper Tongue Member, Paleocene Fort Union Formation, northern Powder River Basin, Wyoming, U.S.A. In: Rahmani, R. A. & Flores, R. M. (eds), *Sedimentology of Coal and Coal-Bearing Sequences. International Association of Sedimentologists, Special Publication*, 7: 85–104.

Gębica, P. & Sokołowski, T., 2001. Sedimentological interpretation of crevasse splays formed during the extreme 1997 flood in the upper Vistula River Valley (south Poland). *Annales Societatis Geologorum Poloniae*, 71: 53–62.

Gębica, P. & Sokołowski, T., 2002. Crevassing of an inland dune during the 1998 flood in upper Vistula river valley (South Poland). *Annales Societatis Geologorum Poloniae*, 72: 191–197.

Gradziński, R., Doktor, M. & Kędzior, A., 2005. Sedimentation of the coal-bearing succession in the Upper Silesia Coal Basin:

research trends and current state of knowledge. *Przegląd Geologiczny*, 53: 734–741. [In Polish, with English abstract.]

Gradziński, R., Doktor, M. & Słomka, T., 1995. Depositional environments of the coal-bearing Cracow Sandstone Series (upper Westphalian), Upper Silesia, Poland. *Studia Geologica Polonica*, 108: 149–170.

Gradziński, R., Kostecka, A., Radomski, A. & Unrug, R., 1976. *Sedymentologia*. Wydawnictwo Geologiczne, Warszawa, 614 pp. [In Polish.]

Guion, P. D., 1984. Crevasse splay deposits and roof-rock quality in the Threequarters Seam (Carboniferous) in the east midlands coalfield, UK. In: Rahmani, R. A. & Flores, R. M. (eds), *Sedimentology of Coal and Coal-Bearing Sequences. International Association of Sedimentologists*, *Special Publication*, 7: 291–308.

Gulliford, A. R., Flint, S. S. & Hodgson, D. M., 2014. Testing applicability of models of distributive fluvial systems or trunk rivers in ephemeral systems: reconstructing 3-D fluvial architecture in the Beaufort Group, South Africa. *Journal of Sedimentary Research*, 84: 1147–1169.

Gulliford, A. R., Flint, S. S. & Hodgson, D. M., 2017. Crevasse splay processes and deposits in an ancient distributive fluvial system: the lower Beaufort Group, South Africa. *Sedimentary Geology*, 358: 1–18.

Hager, H., Kothen, H. & Spann, R., 1981. Zur Setzung der Rheinischen Braunkohle und ihrer klastischen Begleitschichten. *Fortschritte in der Geologie von Rheinland und Westfalen*, 29: 319–352.

Horne, J. C., Ferm, J. C., Caruccio, F. T. & Baganz, B. P., 1978. Depositional models in coal exploration and mine planning in Appalachian region. *American Association of Petroleum Geologists Bulletin*, 62: 2379–2411.

Horner, R. J., McGregor, G. & Holbrook, J., 2018. What's that you splay – A depositional model for the humid terminal splay? A comparative analysis of the modern Rio Seco, Argentina and the Cretaceous-Paleocene Raton Formation, Colorado. In: *AAPG Annual Convention and Exhibition, Salt Lake City, Utah, May 20–23. AAPG Datapages/Search and Discovery Article* #90323.

Jerrett, R. M., Bennie, L. I., Flint, S. S. & Greb, S. F., 2016. Extrinsic and intrinsic controls on mouth bar and mouth bar complex architecture: examples from the Pennsylvanian (upper Carboniferous) of the central Appalachian Basin, Kentucky, USA. *Geological Society of America Bulletin*, 128: 1696–1716.

Jorgensen, P. J. & Fielding, C. R., 1996. Facies architecture of alluvial floodbasin deposits: three-dimensional data from the Upper Triassic Callide Coal Measures of east-central Queensland, Australia. *Sedimentology*, 43: 479–495.

Kasiński, J. R., 1986. Sedimentary models of small lignite deposits: examples from the Polish Neogene. *Przegląd Geologiczny*, 34: 189–197.

Kasiński, J. R., 1989. Lacustrine sedimentary sequences in the Polish Miocene lignite-bearing basins – Facies distribution and sedimentary development. *Palaeoclimatology, Palaeogeography*, *Palaeoecology,* 70: 287–304.

Kędzior, A., 2016. Reconstruction of an early Pennsylvanian fluvial system based on geometry of sandstone bodies and coal seams: the Zabrze Beds of the Upper Silesia Coal Basin, Poland. *Annales Societatis Geologorum Poloniae*, 86: 437–472.

Kędzior, A., Gradziński, R., Doktor, M. & Gmur, D., 2007. Sedimentary history of a Mississippian to Pennsylvanian coal-bearing succession: an example from the Upper Silesia Coal Basin, Poland. *Geological Magazine*, 144: 487–496.

Kędzior, A., Widera, M. & Zieliński, T., 2021. Ancient and modern anastomosing rivers: insights from sedimentological and geomorphological case studies of the Triassic, Neogene and Holocene of Poland. *Geological Quarterly*, 65: 54.

Kłosowski, S., Jabłońska, E. & Szańkowski, M., 2011. Aquatic vegetation as an indicator of littoral habitats and various stages of lake aging in north-eastern Poland. *International Journal of Limnology*, 47: 281–295.

Kordowski, J., Gamrat, W., Gierszewski, P., Kubiak-Wójcicka, K., Szmańda, J., Tyszkowski, S. & Solarczyk, A., 2014. Record of fluvial and biogenic sedimentation processes in sediments of the Lower Vistula Valley floor. *Landform Analysis*, 25: 77–93. [In Polish, with English abstract.]

Kramarska, R., Kasiński, J. R., Czapowski, G., Piwocki, M. & Słodkowska, B., 2015. The standard section of Neogene deposits from Eastern Pomerania at Łęczyce near Lębork (Northern Poland)]. *Biuletyn Państwowego Instytutu Geologicznego*, 461: 193–250. [In Polish, with English abstract.]

Kraus, M. J. & Wells, T. M., 1999. Recognizing avulsion deposits in the ancient stratigraphical record. In: Smith, N. D. & Rogers, J. (eds), *Fluvial Sedimentology VI. Special Publication of the International Association of Sedimentologists*, 28: 251–268.

Kwiecińska, B. & Wagner, M., 1997. *Classification of Qualitative Features of Brown Coal from Polish Deposits According to Petrographical, Chemical and Technological Criteria.* Wydawnictwo Centrum PPGSMiE Polskiej Akademii Nauk, Kraków, 87 pp. [In Polish, with English abstract.]

Lepre, C. J., 2017. Crevasse splay and associated depositional environments of the hominin bearing lower Okote Mbr, Koobi Fora Fm (Plio-Pleistocene) Kenya. *The Depositional Record*, 3: 161–186.

Lewin, J., Ashworth, P. J. & Strick, R. J. P., 2017. Spillage sedimentation on large river floodplains. *Earth Surface Processes and Landforms*, 42: 290–305.

Mach, K., Sýkorová, I., Konzalová, M. & Opluštil, S., 2013. Effect of relative lake-level changes in mire-lake system on the petrographic and floristic compositions of a coal seam, in the Most Basin (Miocene), Czech Republic. *International Journal of Coal Geology*, 105: 120–136.

Maciaszek, P., Chomiak, L., Urbański, P. & Widera, M., 2020. New insights into the genesis of the 'Poznań Clay' – upper Neogene of Poland. *Civil and Environmental Engineering Reports*, 30: 18–32.

Makaske, B., 2001. Anastomosing rivers: a review of their classification, origin and sedimentary products. *Earth-Science Reviews*, 53: 149–196.

Markič, M. & Sachsenhofer, R. F., 1997. Petrographic composition and depositional environments of the Pliocene Velenje lignite seam (Slovenia). *International Journal of Coal Geology*, 33: 229–254.

McCabe, P. J., 1984. Depositional models of coal and coal-bearing strata. In: Rahmani, R. A. & Flores, R. M. (eds), *Sedimentology of Coal and Coal-Bearing Sequences.*

International Association of Sedimentologists, *Special Publication*, 7: 13–42.

McKee, E. D., Crosby, E. J. & Berryhill, H. I., Jr., 1967. Flood deposits, Bijou Creek, Colorado. June 1965. *Journal of Sedimentary Petrology,* 37: 829–851.

Miall, A. D., 1977. A review of the braided-river depositional environment. *Earth-Science Reviews*, 13: 1–62.

Miall, A. D., 2006. *The Geology of Fluvial Deposits*. *4th ed.* Springer-Verlag, Berlin, 582 pp.

Michaelsen, P., Henderson, R. A., Crosdale, P. J. & Mikkelsen, S. O., 2000. Facies architecture and depositional dynamics of the Upper Permian Rangal Coal Measures, Bowen Basin, Australia. *Journal of Sedimentary Research*, 70: 879–895.

Millard, C., Hajek, E. & Edmonds, D. A., 2017. Evaluating controls on crevasse-splay size: Implications for floodplain-basin filling. *Journal of Sedimentary Research*, 87: 722–739.

Mjøs, R., Walderhaug, O. & Prestholm, E., 1993. Crevasse-splay sandstone geometries in the Middle Jurassic Ravenscar Group of Yorkshire, UK. In: Marzo, M. & Puigdefabregas, C. (eds), *Alluvial Sedimentation. International Association of Sedimentologists*, *Special Publication*, 17: 167–184.

Morozova, G. S. & Smith, N. D., 2000. Holocene avulsion styles and sedimentation patterns of the Saskatchewan River, Cumberland Marshes, Canada. *Sedimentary Geology*, 130: 81–105.

Nemec, W., 1984. Wałbrzych Beds (Lower Namurian, Wałbrzych Coal Basin): analysis of alluvial sedimentation in a coal basin. *Geologia Sudetica*, 19: 7–73. [In Polish, with English abstract.]

Nemec, W., 2009. What is a hyperconcentrated flow? In: *Lecture Abstracts, 27th IAS Annual Meeting. Alghero, Italy*. Medimond, Bologna, p. 293.

O'Brien, P. E. & Wells, A. T., 1986. A small, alluvial crevasse splay. *Journal of Sedimentary Research*, 56: 876–879.

Pieńkowski, G., 2004a. Sołtyków, Poland – an unique palaeoecological record of the Early Jurassic continental deposits. *Volumina Jurassica*, 2: 1–16. [In Polish, with English abstract.]

Pieńkowski, G., 2004b. The epicontinental Lower Jurassic of Poland. *Polish Geological Institute Special Papers*, 12: 1–152.

Pierson, T. C., 2005. Hyperconcentrated flow – transitional process between water flow and debris flow. In: Jakob, M. & Hungr, O. (eds), *Debris-flow Hazards and Related Phenomena*. Springer-Verlag Praxis Books, Berlin, pp. 159–202.

Piwocki, M., 1992. Extent and correlations of main groups of the Tertiary lignite seams on Polish platform area. *Przegląd Geologiczny*, 40: 281–286. [In Polish, with English abstract.]

Piwocki, M. & Ziembińska-Tworzydło, M., 1997. Neogene of the Polish Lowlands – lithostratigraphy and pollen-spore zones. *Geological Quarterly*, 41: 21–40.

Rahman, M. M., Howell, J. A. & Macdonald, D. I. M., 2022a. Quantitative analysis of crevasse-splay systems from modern fluvial settings. *Journal of Sedimentary Research*, 92: 751–774.

Rahman, M. M., Howell, J. A. & Macdonald, D. I. M., 2022b. Virtual outcrop-based analysis of channel and crevasse splay sandstone body architecture in the Middle Jurassic Ravenscar Group, Yorkshire, NE England. *Journal of Geological Society,* 179: jgs2021-017.

Rajchl, M. & Uličný, D., 2005. Depositional record of an avulsive fluvial system controlled by peat compaction (Neogene, Most Basin, Czech Republic). *Sedimentology*, 52: 601–625.

Rajchl, M., Uličný, D. & Mach, K., 2008. Interplay between tectonics and compaction in a rift-margin, lacustrine delta system: Miocene of the Eger Graben, Czech Republic. S*edimentology*, 55: 1419–1447.

Reading, H. G. & Collinson, J. D., 1996. Clastic coasts. In: Reading, H. G. (ed.), *Sedimentary Environments: Processes, Facies, and Stratigraphy*. *3rd ed*., Blackwell, London, pp. 154–232.

Słodkowska, B. & Widera, M., 2021. Vegetation response to environmental changes based on palynological research on the Middle Miocene lignite at the Jóźwin IIB open-cast mine (Konin region, central Poland). *Annales Societatis Geologorum Poloniae*, 91: 149–166.

Słodkowska, B. & Widera, M., 2022. Reconstruction of the sedimentary environment of phytogenic deposits in the Tomisławice open cast mine (Konin Region, central Poland). *Geological Quarterly*, 66: 34.

Smith, N. D., Cross, T. A., Dufficy, J. P. & Clough, S. R., 1989. Anatomy of an avulsion. *Sedimentology*, 36: 1–23.

Szponar, A., 2000. Overbank deposits of Odra river during the 1997 flood. *Przegląd Geologiczny*, 48: 176–181. [In Polish, with English abstract.]

Teichmüller, M., 1958. Rekonstruktion verschiedener Moortypen des Hauptflözes der niederrheinischen Braunkohle. *Fortschrift in der Geologie von Rheinland und Westfalen*, 2: 599–612.

Teichmüller, M., 1989. The genesis of coal from the viewpoint of coal petrology. *International Journal of Coal Geology*, 12: 1–87.

Teisseyre, A. K., 1985. Recent overbank deposits of the Sudetic valleys, SW Poland. Part I: general environmental characteristics (with examples from the upper River Bóbr drainage basin). *Geologia Sudetica*, 20: 113–195. [In Polish, with English abstract.]

Ticleanu, N., Scradeanu, D., Popa, M., Milutinovici, S., Popa, R., Preda, I., Ticleanu, M., Savu, C., Diaconita, D., Barus, T., Petrescu, I., Dinulescu, C. & Maftei, R., 1999. The relation between the lithotypes of Pliocene coals from Oltenia and their main quality characteristics. *Bulletin of the Czech Geological Survey*, 74: 169–174.

Tye, R. S. & Coleman, J. M., 1989. Evolution of Atchafalaya lacustrine deltas, south-central Louisiana. *Sedimentary Geology*, 65: 95–112.

Van Toorenenburg, K. A., Donselaar, M. E., Noordijk, N. A. & Weltje, G. J., 2016. On the origin of crevasse-splay amalgamation in the Huesca fluvial fan (Ebro Basin, Spain): implications for connectivity in low net-to-gross fluvial deposits. *Sedimentary Geology*, 343: 156–164.

Wachocki, R., Chomiak, L. & Widera, M., 2020. Tectonic and sedimentary deformational structures within the first Mid-Polish lignite seam – Konin Basin, central Poland. *IOP Conference Series: Earth and Environmental Science*, 609: 012019.

Wang, J., Guan, Z., La Croix, A. D., Wang, Q., Ji, L. & Sun, J., 2020. Seismic geomorphology of shallow-water lacustrine deltas in the Paleocene Huanghua Depression, Bohai Bay Basin, eastern China. *Marine and Petroleum Geology*, 120: 104561.

Widera, M., 1998. Palaeomorphological and palaeotectonical evolution of the Konin Elevation. *Geologos*, 3: 55–103. [In Polish, with English abstract.]

Widera, M., 2007. *Lithostratigraphy and Palaeotectonics of the sub-Pleistocene Cenozoic of Wielkopolska*. Adam Mickiewicz University Press, Poznań, 224 pp. [In Polish, with English abstract.]

Widera, M., 2012. Macroscopic lithotype characterisation of the 1st Middle-Polish (1st Lusatian) Lignite Seam in the Miocene of central Poland. *Geologos*, 18: 1–11.

Widera, M., 2013a. Sand- and mud-filled fluvial palaeochannels in the Wielkopolska Member of the Neogene Poznań Formation, central Poland. *Annales Societatis Geologorum Poloniae*, 83: 19–28.

Widera, M., 2013b. Changes of the lignite seam architecture – a case study from Polish lignite deposits. *International Journal of Coal Geology*, 114: 60–73.

Widera, M., 2015. Compaction of lignite: a review of methods and results. *Acta Geologica Polonica*, 65: 367–368.

Widera, M., 2016a. Depositional environments of overbank sedimentation in the lignite-bearing Grey Clays Member: new evidence from Middle Miocene deposits of central Poland. *Sedimentary Geology*, 335: 150–165.

Widera, M., 2016b. An overview of lithotype associations forming the exploited lignite seams in Poland. *Geologos*, 22: 213–225.

Widera, M., 2017. Sedimentary breccia formed atop a Miocene crevasse-splay succession in central Poland. *Sedimentary Geology*, 360: 96–104.

Widera, M., 2020. Slump folds within mid-Miocene crevasse-splay deposits: a unique example from the Tomisławice lignite opencast mine in central Poland. *Geological Quarterly*, 64: 711–722.

Widera, M., 2021. *Geologia polskich złóż węgla brunatnego*. Bogucki Wydawnictwo Naukowe, Poznań, 180 pp. [In Polish.]

Widera, M., 2022. *Zarys geologii okolic Poznania, Turku i Konina*. Bogucki Wydawnictwo Naukowe, Poznań, 97 pp. [In Polish.]

Widera, M., Bechtel, A., Chomiak, L., Maciaszek, P., Słodkowska, B., Wachocki, R., Worobiec, E., Worobiec, G. & Zieliński, T., 2021a. Palaeoenvironmental reconstruction of the Konin Basin (central Poland) during lignite accumulation linked to the Mid-Miocene Climate Optimum. *Palaeogeography, Palaeoclimatology, Palaeoecology,* 568: 110307.

Widera, M., Chomiak, L., Gradecki, D. & Wachocki, R., 2017a. Crevasse splay deposits from the Miocene of central Poland near Konin. *Przegląd Geologiczny*, 65: 251–258. [In Polish, with English abstract.]

Widera, M., Chomiak, L. & Wachocki, R., 2023. Distinct types of crevasse splays formed in the area of Middle Miocene mires, central Poland: Insights from geological mapping and facies analysis. *Sedimentary Geology*, 443: 106300.

Widera, M., Chomiak, L. & Zieliński, T., 2019. Sedimentary facies, processes and paleochannel pattern of an anastomosing river system: an example from the Upper Neogene of Central Poland. *Journal of Sedimentary Research*, 89: 487–507.

Widera, M., Glacová, V. & Marschalko, M., 2022. Origin of clastic partings and their impact on ash yield in mined lignite: A case study from Middle Miocene of central Poland. *Journal of Cleaner Production*, 378: 134401.

Widera, M., Jachna-Filipczuk, G., Kozula, R. & Mazurek, S., 2007. From peat bog to lignite seam: a new method to calculate the consolidation coefficient of lignite seams, Wielkopolska region in central Poland. *International Journal of Earth Sciences*, 96: 947–955.

Widera, M., Kowalska, E. & Fortuna, M., 2017b. A Miocene anastomosing river system in the area of Konin Lignite Mine, central Poland. *Annales Societatis Geologorum Poloniae*, 87: 157–168.

Widera, M., Zieliński, T., Chomiak, L., Maciaszek, P., Wachocki, R., Bechtel, A., Słodkowska, B., Worobiec, E. & Worobiec, G., 2021b. Tectonic-climatic interactions during changes of depositional environments in the Carpathian foreland: An example from the Neogene of central Poland. *Acta Geologica Polonica*, 71: 519–542.

Worobiec, E., Widera, M. & Worobiec, G., 2022. Palaeoenvironment of the middle Miocene wetlands at Drzewce, Konin region, central Poland. *Annales Societatis Geologorum Poloniae*, 92: 201–218.

Worobiec, E., Widera, M., Worobiec, G. & Kurdziel, B., 2021. Middle Miocene palynoflora from the Adamów lignite deposit, central Poland. *Palynology*, 45: 59–71.

Zagwijn, W. H. & Hager, H., 1987. Correlations of continental and marine Neogene deposits in the south-eastern Netherlands and the Lower Rhine District. *Mededelingen van de Werkgroep voor Tertiaire en Kwartaire Geologie*, 24: 59–78.

Zieliński, T., 2014. *Sedymentologia. Osady rzek i jezior*. Wydawnictwo Naukowe UAM, Poznań, 594 pp. [In Polish.]

Zieliński, T. & Widera, M., 2020. Anastomosing-to-meandering transitional river in sedimentary record: A case study from the Neogene of central Poland. *Sedimentary Geology*, 404: 105677.

Zwoliński, Z., 1985. Sedymentacja osadów przyrostu pionowego na terasie zalewowej Parsęty. *Badania Fizjograficzne nad Polską Zachodnią*, 35A: 205–238. [In Polish.]

Zwoliński, Z., 1992. Sedimentology and geomorphology of overbank flows on meandering river floodplains. *Geomorphology*, 4: 367–379.

Żelaźniewicz, A., Aleksandrowski, P., Buła, Z., Karnkowski, P. H., Konon, A., Oszczypko, N., Ślączka, A., Żaba, J. & Żytko, K., 2011. *Regionalizacja tektoniczna Polski*. Komitet Nauk Geologicznych Polska Akademia Nauk, Wrocław, 60 pp. [In Polish.]

Appendix

Examples of cross-stratified facies at various scales within the sandy complex examined (**A, B**), as well as 'grey clay' – Grey Clay Member; 'green clay' and 'flamy clay' – Wielkopolska Member (**C**), documented during supplementary field research in August and September 2022. For an explanation of facies codes, see Table 2.